

Electronic Supplementary Information for

**A multi-responsive luminescent sensor based on a super-stable sandwich-type
terbium(III)-organic framework**

Guo-Xuan Wen^{#,a}, Min-Le Han^{#,a,b}, Xue-Qian Wu^a, Ya-Pan Wu^a, Wen-Wen Dong^a, Jun Zhao^a,
Dong-Sheng Li^{*,a} and Lu-Fang Ma^{*,b}

^a College of Materials & Chemical Engineering, Collaborative Innovation Centre for Microgrid of New Energy of Hubei Province, Key laboratory of inorganic nonmetallic crystalline and energy conversion materials, China Three Gorges University, Yichang, 443002, China. Tel./Fax: +86-717-6397506; E-mail address: lidongsheng1@126.com (D.-S. Li).

^b College of Chemistry and Chemical Engineering, and Henan Key Laboratory of Function-Oriented Porous Materials, Luoyang Normal University, Luoyang 471934, P. R. China. E-mail address: mazhuxp@126.com (L.-F. Ma).

Table S1. Selected Bond Lengths (\AA) and Angles ($^\circ$) for **Tb-MOF**.

Tb(1)-O(2)#1	2.312(3)	Tb(1)-O(4)#1	2.329(3)
Tb(1)-O(3)	2.337(3)	Tb(1)-O(1)	2.400(3)
Tb(1)-O(5)#2	2.405(3)	Tb(1)-O(8)	2.413(3)
Tb(1)-O(7)	2.450(3)	Tb(1)-O(6)#2	2.476(3)
O(2)#1-Tb(1)-O(4)#1	71.36(10)	O(2)#1-Tb(1)-O(3)	82.08(11)
O(4)#1-Tb(1)-O(3)	129.55(10)	O(2)#1-Tb(1)-O(1)	124.70(11)
O(4)#1-Tb(1)-O(1)	79.86(10)	O(3)-Tb(1)-O(1)	81.50(11)
O(2)#1-Tb(1)-O(5)#2	79.22(13)	O(3)-Tb(1)-O(5)#2	79.56(11)
O(4)#1-Tb(1)-O(5)#2	132.89(10)	O(8)-Tb(1)-O(6)#2	70.48(10)
O(3)-Tb(1)-O(8)	139.59(10)	O(1)-Tb(1)-O(8)	72.27(10)
O(2)#1-Tb(1)-O(8)	138.22(10)	O(4)#1-Tb(1)-O(8)	75.82(10)
O(5)#2-Tb(1)-O(8)	106.44(12)	O(2)#1-Tb(1)-O(7)	146.82(11)
O(1)-Tb(1)-O(7)	74.35(11)	O(5)#2-Tb(1)-O(7)	74.28(12)
O(4)#1-Tb(1)-O(7)	141.82(10)	O(3)-Tb(1)-O(7)	73.86(10)
O(8)-Tb(1)-O(7)	69.83(10)	O(2)#1-Tb(1)-O(6)#2	82.09(10)
O(4)#1-Tb(1)-O(6)#2	86.15(9)	O(3)-Tb(1)-O(6)#2	132.35(10)
O(1)-Tb(1)-O(6)#2	142.37(10)	O(5)#2-Tb(1)-O(6)#2	53.40(10)
O(1)-Tb(1)-O(5)#2	146.77(11)	O(7)-Tb(1)-O(6)#2	97.39(10)

Symmetry codes: #1, -x + 2, -y, -z; #2, x + 1/2, -y + 1/2, z + 1/2.

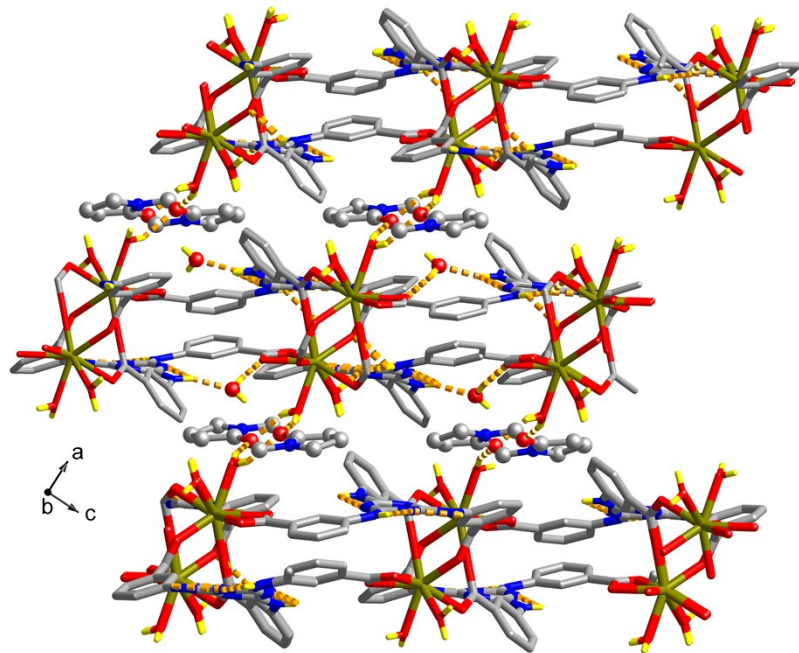


Fig. S1. 3D sandwich-type supramolecular net of **Tb-MOF**. Hydrogen bonds are represented as light orange dash line.

Table S2. Distance (\AA) and angles ($^\circ$) of hydrogen bonding for **Tb-MOF**.

D-H \cdots A	d(D-H)	d(H \cdots A)	d(D \cdots A)	\angle (DHA)
O(7)-H(7A) \cdots O(9)#3	0.85	2.041	2.799	148.22
O(7)-H(7B) \cdots O(9)#4	0.85	1.961	2.784	162.62
O(8)-H(8A) \cdots N(3)#5	0.85	1.880	2.704	162.75
O(10)-H(10A) \cdots O5#6	0.850	2.056	2.889	166.48
N(1)-H(1) \cdots O(10)#6	0.860	2.025	2.863	164.60
N(6)-H(6) \cdots O(4)#6	0.860	2.263	2.931	134.55

Symmetry codes: #3, x + 1, y - 1, z; #4, -x + 2, -y + 1, -z; #5, x, y - 1, z; #6, -x + 2, -y + 1, -z.

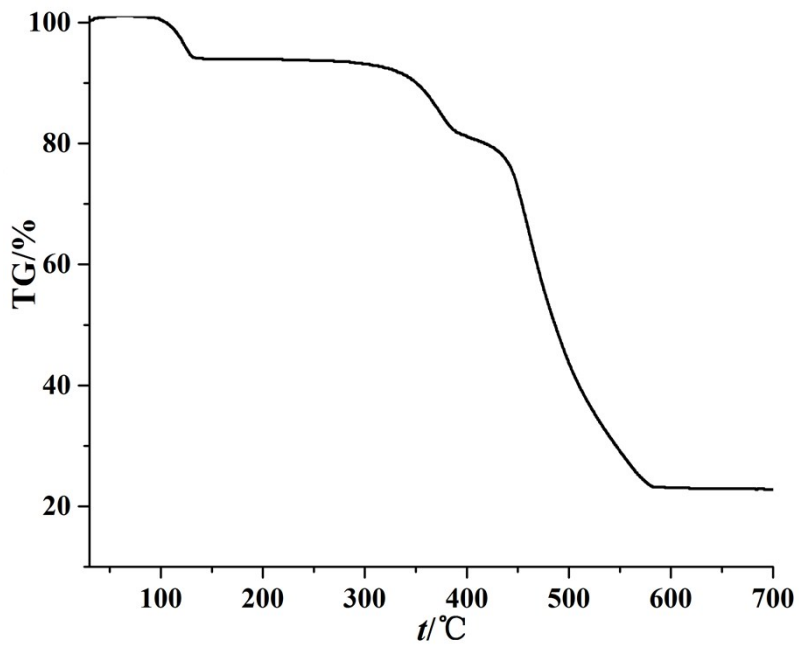


Fig. S2. TGA plot of complexes **Tb-MOF**. For **Tb-MOF**, the first weight loss of 6.9% (calcd. 6.8%) was observed from 92 to 132 °C corresponding to the loss of free and coordinated water molecules. The second weight loss of 12.2% (calcd. 11.9%) might start from 283 to 391 °C, indicating the loss of NMP molecules. Then the framework collapsed in the temperature range 392-582 °C before the final formation of the Tb_2O_3 (calc. 23.0%, exp. 23.2%).

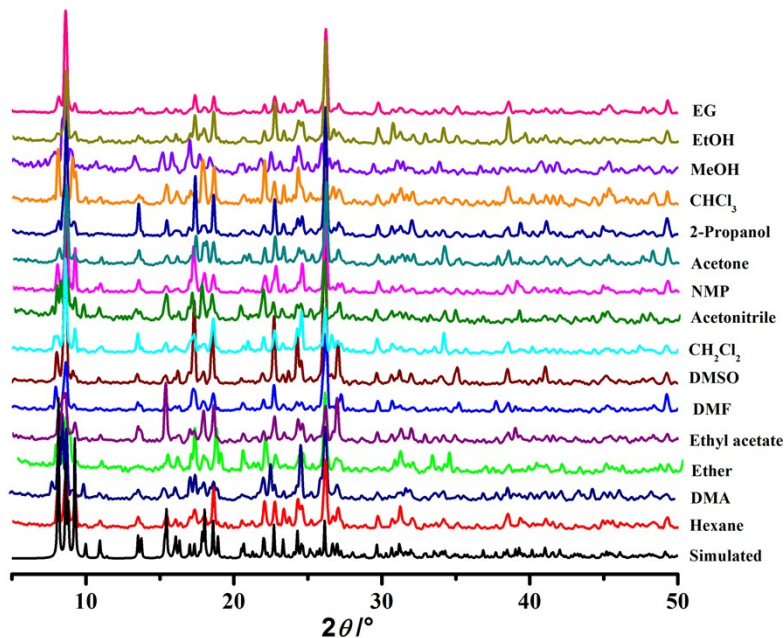


Fig. S3. PXRD patterns of **Tb-MOF**; the simulated, and immersed in organic solvent for one month.

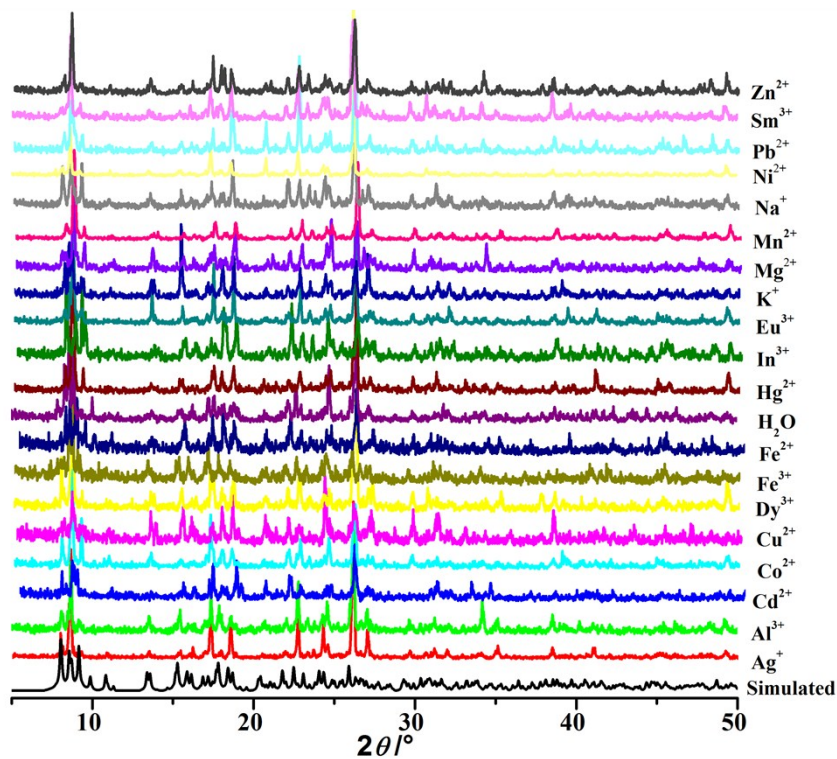


Fig. S4. PXRD patterns of **Tb-MOF**; the simulated, as-synthesized, immersed in H_2O solutions containing different M^{k+} (10^{-2} M) for three days.

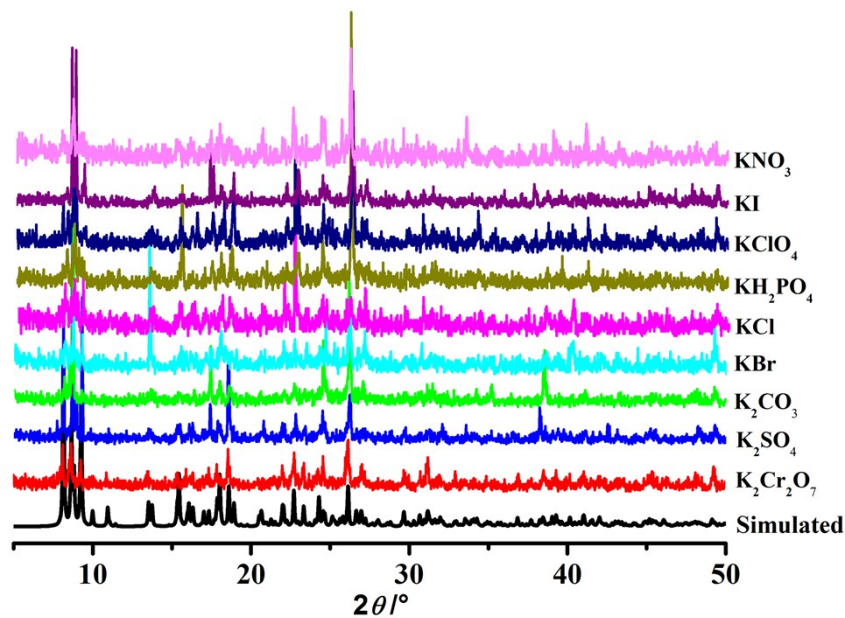


Fig. S5. PXRD patterns of **Tb-MOF**; the simulated, as-synthesized, immersed in H_2O solutions containing different X^{l-} (10^{-2} M) for three days.

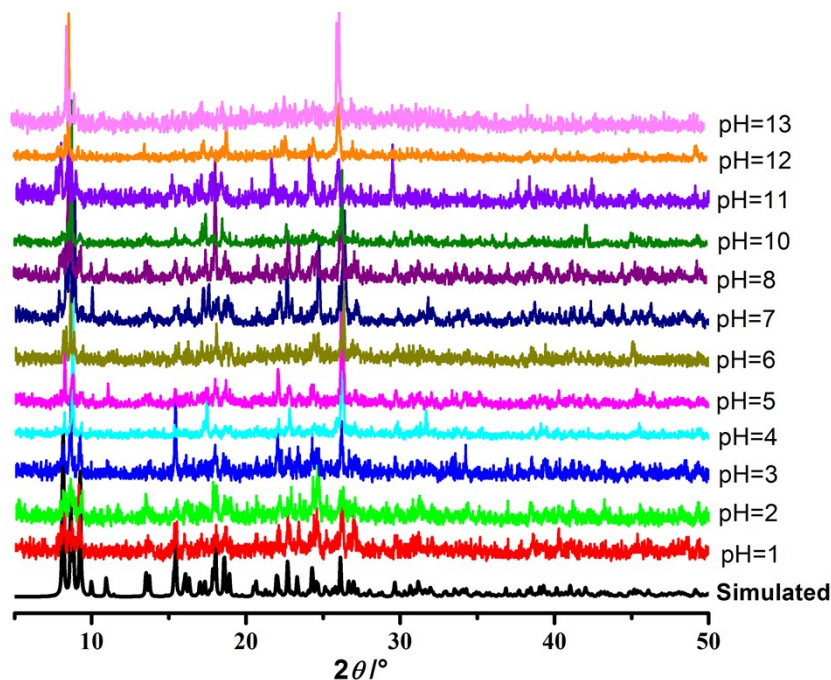


Fig. S6. PXRD patterns of **Tb-MOF**; the simulated, as-synthesized, immersed in H_2O solutions with different pH values.

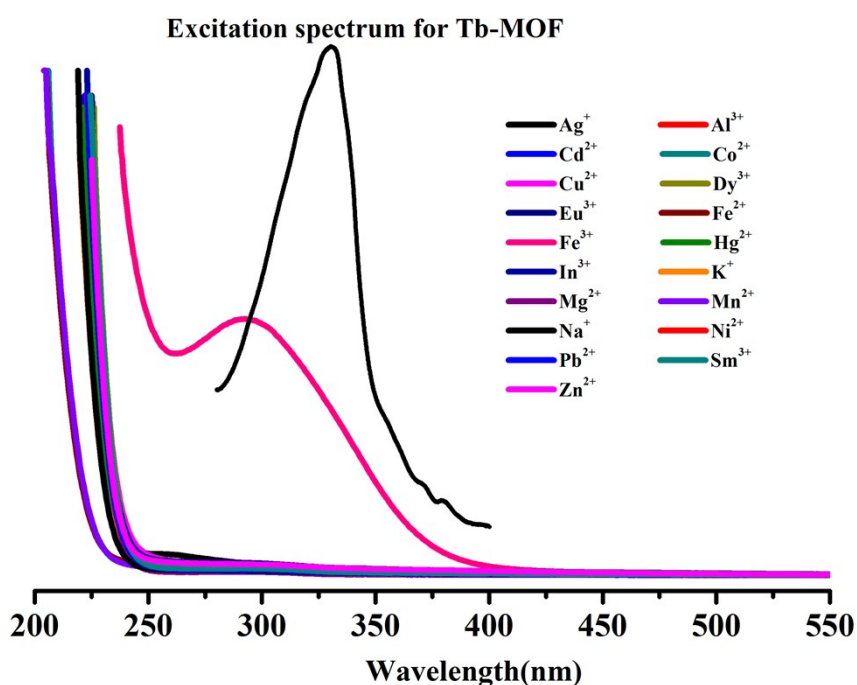


Fig. S7. The UV-vis absorption spectra of metal cations aqueous solution with the same concentration of analytes (0.01 M) and the excitation spectra of **Tb-MOF**.

Excitation spectrum for Tb-MOF

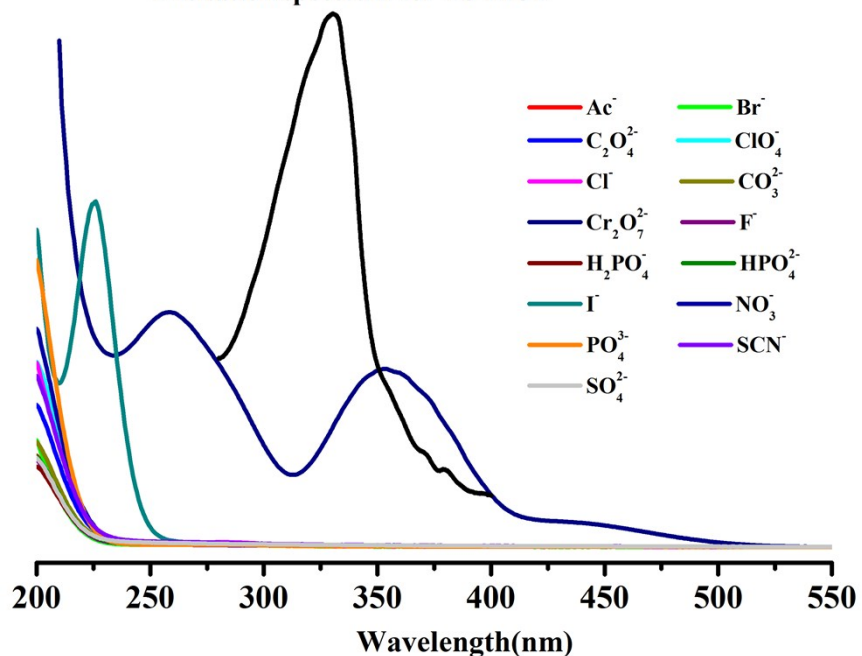


Fig. S8. The UV-vis absorption spectra of inorganic anions aqueous solution with the same concentration of analytes (0.01 M) and the excitation spectra of **Tb-MOF**.

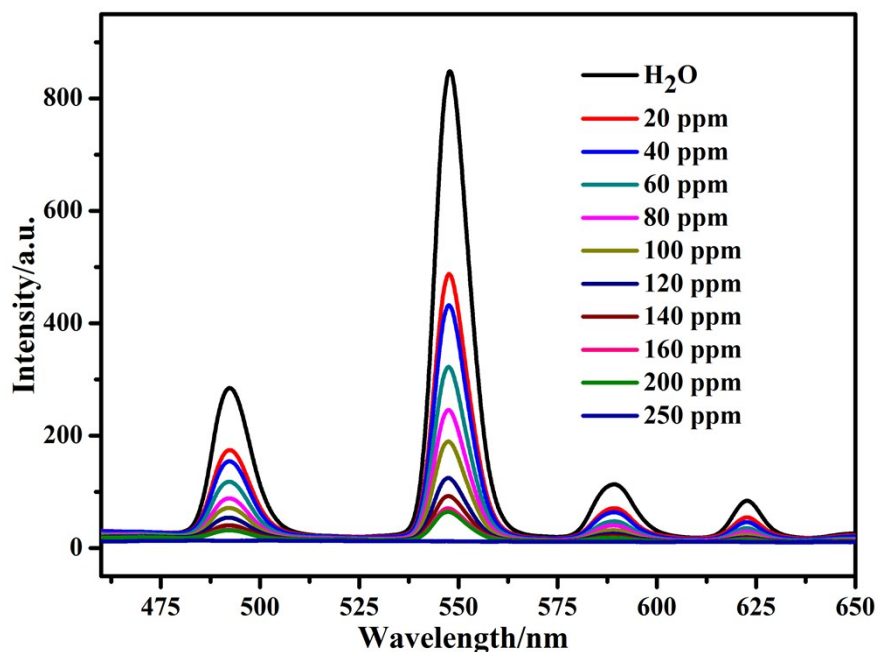


Fig. S9. Luminescence spectra of **Tb-MOF** with 2-NP at different concentrations in water solution.

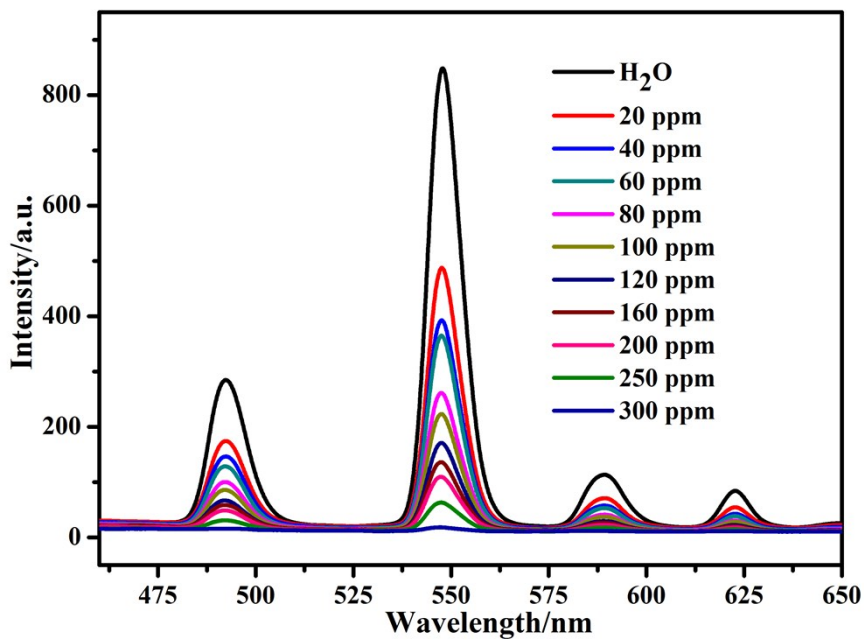


Fig. S10. Luminescence spectra of **Tb-MOF** with 3-NP at different concentrations in water solution.

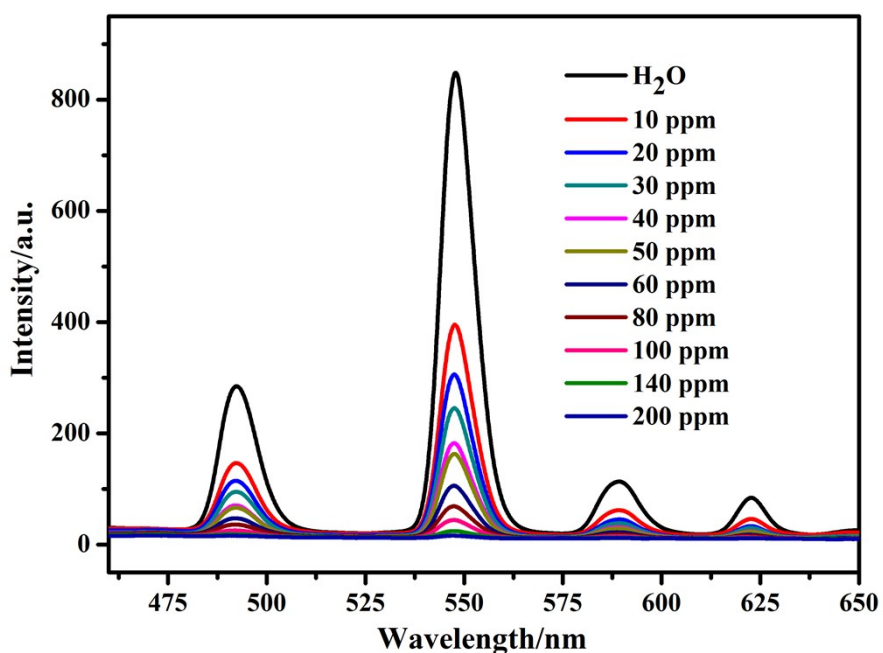


Fig. S11. Luminescence spectra of **Tb-MOF** with 4-NP at different concentrations in water solution.

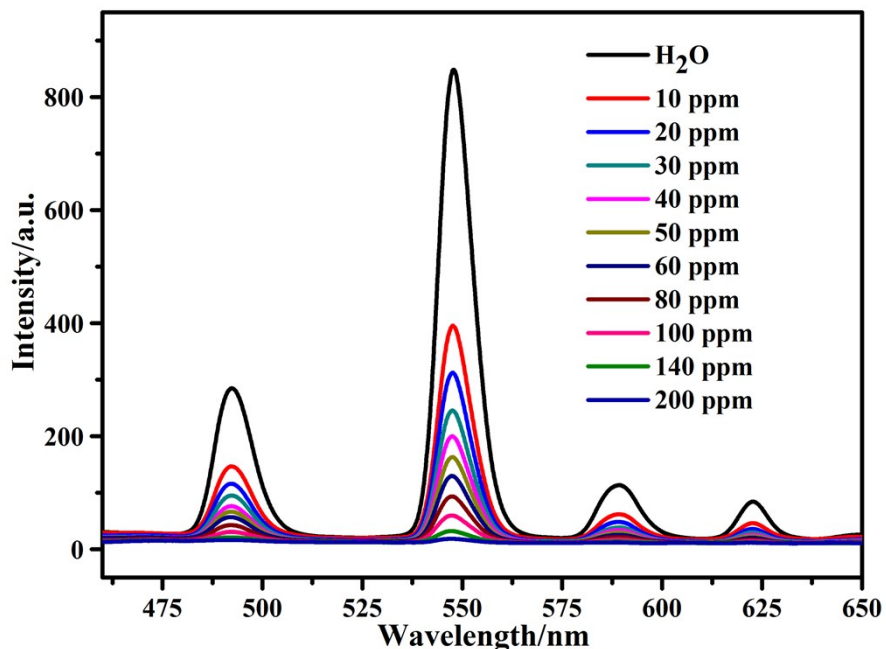


Fig. S12. Luminescence spectra of **Tb-MOF** with TNP at different concentrations in water solution.